

Heterogeneous Catalysis

Single Crystal to Single Crystal (SC-to-SC) Transformation from a Nonporous to Porous Metal–Organic Framework and Its Application Potential in Gas Adsorption and Suzuki Coupling Reaction through Postmodification

Rupam Sen,^{*[a, c]} Debraj Saha,^[b] Subratanath Koner,^[b] Paula Brandão,^[a] and Zhi Lin^{*[a]}

Abstract: A new amino-functionalized strontium–carboxylate-based metal–organic framework (MOF) has been synthesized that undergoes single crystal to single crystal (SC-to-SC) transformation upon desolvation. Both structures have been characterized by single-crystal X-ray analysis. The desolvated structure shows an interesting 3D porous structure with pendent –NH₂ groups inside the pore wall, whereas the solvated compound possesses a nonporous structure with DMF molecules on the metal centers. The amino group was postmodified through Schiff base condensation by

pyridine-2-carboxaldehyde and palladium was anchored on that site. The modified framework has been utilized for the Suzuki cross-coupling reaction. The compound shows high activity towards the C–C cross-coupling reaction with good yields and turnover frequencies. Gas adsorption studies showed that the desolvated compound had permanent porosity and was microporous in nature with a BET surface area of 2052 m²g^{−1}. The material also possesses good CO₂ (8 wt%) and H₂ (1.87 wt%) adsorption capabilities.

Introduction

Rapid development has been achieved on the synthesis and application of metal–organic frameworks (MOFs) during the last decade. Much effort has been invested in the rational design of MOF materials in the fields of gas adsorption and storage, catalysis, and magnetic material synthesis.^[1–3] Many different pathways have been adopted to produce different MOFs based on their applications. Among the different strategies used, postsynthetic modification (PSM) of the MOFs

is a convenient and unique tool to produce MOFs with novel applicability. Since the evolution of the isorecticular synthesis of MOFs, syntheses by modulating the bridging ligands are now of paramount interest to synthetic inorganic chemists.^[4] It is worth mentioning that MOFs with large pore and functionalizable bridging arms are of wide interest due to their varied applications from catalysis to gas adsorption. It is well reported that bifunctional dicarboxylates serve to bridge various metal ions, producing many highly porous and catalytically active frameworks.^[5] By tuning the porous channel, one can rationalize the adsorption and catalytic properties within the pores of materials.

In catalytic reactions, palladium-catalyzed cross-coupling is one of the most powerful tools for the formation of C–C bonds in organic synthesis.^[6] There are many approaches, including Suzuki, Stille, and Sonogashira, that are well recognized and highly applicable in organic synthesis.^[7] Among them, the Suzuki coupling reaction has become a mainstay in modern synthetic organic chemistry for the preparation of biaryl compounds in a feasible manner, and researchers are still engaged in developing this field to make it more cost effective and truly heterogeneous.^[8] The coupling products of these reactions have been employed in a variety of applications as intermediates in the preparation of functional materials, natural products, and bioactive compounds.^[9] It is worth mentioning that recently scientists have used this technique to produce different bridging ligands to construct porous and functionalizable MOFs.^[10] Although homogeneous catalytic systems are known to exhibit better activity than heterogeneous systems, for large-scale applications in liquid-phase reactions

[a] Dr. R. Sen, Dr. P. Brandão, Dr. Z. Lin
Department of Chemistry, CICECO, University of Aveiro
3810-193 Aveiro (Portugal)
E-mail: rupamsen1@yahoo.com
zlin@ua.pt

[b] D. Saha, Dr. S. Koner
Department of Chemistry, Jadavpur University
Kolkata 700 032 (India)

[c] Dr. R. Sen
Present address: Institute for Materials Chemistry and Engineering
Kyushu University, Kasuga, Fukuoka 816-8580 (Japan)

Supporting information for this article is available on the WWW under <http://dx.doi.org/10.1002/chem.201405684>. It contains detailed experimental information; crystal structure refinement parameters and tables for bond distances and angles; cif; a scheme for the three-phase and blank tests; the solid-state UV/Vis spectrum of the catalyst; powder XRD patterns of Sr-MOF-1, Sr-MOF-1-PI, and Sr-MOF-1-PI-Pd, TG analysis and differential thermal analysis profiles of Sr-MOF-1; SEM images and X-ray elemental mapping of Sr-MOF-1, Sr-MOF-1-PI, Sr-MOF-1-PI-Pd, and the recovered catalyst; powder XRD patterns; gas adsorption studies of virgin and recovered catalyst, plots for the comparison of the percentage conversion in C–C coupling reactions with different amounts of SH–SiO₂; and ¹H NMR spectra of all products of known compounds.

they causes greater difficulties, such as purification of the final product, recycling of the catalyst, and deactivation of catalyst through aggregation of inactive palladium particles. Further removal of palladium from organic products at the end of the reaction is highly desirable because of its high cost and toxicity. Hence, the development of heterogeneous systems in which the metal is grafted onto inorganic or organic supports has attracted attention in recent years.^[11]

Recently, a few approaches have been made to use MOFs in catalysis.^[9–13] After the first introduction of PSM by Seo and co-workers, the field opened up to a new strategy of using MOFs in catalytic reactions.^[12b] In another study, Cohen et al.^[12c] successfully developed the postmodification of IRMOF-3 and covalently modified the pendant $-\text{NH}_2$ linkers to amides by more than $>80\%$. Since then, many organic reactions have been used to covalently functionalize MOF backbones.^[9–13] Thus, these MOFs represent a good model system for postsynthetic covalent modification studies. However, heavy-metal-anchored MOFs are still scarce in this field.^[10,14] Therefore, new strategies to develop such catalytic systems and exploit their remarkable structural and chemical flexibility deserve to be explored in more detail. In the course of our continuing investigations into the catalytic uses of MOFs, we have successfully employed

layered metal carboxylates and vanadium(IV) hydrogen phosphate and lanthanide-based MOFs to catalyze the olefin epoxidation reaction under heterogeneous conditions.^[15] Recently, we developed porous MOF-based catalysts containing alkaline-earth metals for aldol condensation reactions.^[16] In contrast to those systems, herein, we introduce a novel strontium-based MOF that is highly thermally and chemically robust, can be postfunctionalized by covalent modification, and can also be used for Suzuki cross-coupling reactions by anchoring palladium onto the modified arms. In addition to C–C coupling reactions, the structure also possesses permanent porosity and shows good H_2 and CO_2 adsorption properties. To the best of our knowledge, this is the first example of alkaline-earth-based MOFs for postmodification. It is also the first reported strontium-based MOF with the highest low pressure H_2 and CO_2 adsorption capacities at 77 and 298 K, respectively.

Results and Discussion

Structural description of Sr-MOF-1'

The compound crystallizes in the space group $P2_1/n$ with a Z value of four. This compound possesses an extended 3D structure. The asymmetric units are formed by one Sr ion, one amino terephthalate anion (ATA), and one μ_2 -bridged DMF molecule. In the asymmetric unit, each metal center is a monocapped pentagonal bipyramid that shares edges to create an inorganic motif in the form of a zigzag 1D chain running along the b axis. The basal plane is formed by five oxygen atoms (O8, O8[#], O15, O15[#], O9; in which $\# = -\frac{1}{2} + x, -\frac{1}{2} - y, -\frac{1}{2} + z$) and the axial sites are fulfilled by oxygen atoms (O1 and O2). The monocapped position is occupied by O1* (the coordination environment is shown in Figure 1a). These 1D chains are

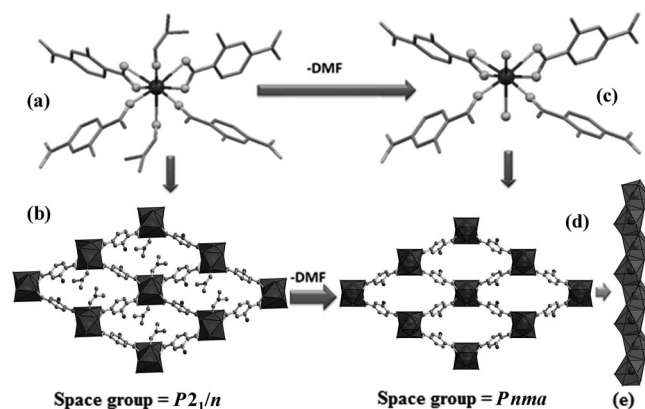


Figure 1. Single-crystal X-ray structures: a) coordination environment of Sr-MOF-1'; b) 3D packing diagram of Sr-MOF-1', showing the DMF molecules present inside the pores of the MOF; c) coordination environment of Sr-MOF-1; d) 3D porous structure of Sr-MOF-1 without DMF molecules; and e) 1D edge-shared chain present in both compounds.

connected by the μ links of the ATA ligands in two directions to generate the 3D framework. The pores of the 3D structure are filled with DMF molecules and the walls are decorated with free $-\text{NH}_2$ groups (Figure 1b). A solvent-accessible void (SAV) calculation by PLATON analysis shows no SAV.

Structural description of Sr-MOF-1

On the other hand, single-crystal X-ray diffraction shows that the desolvated structure crystallizes in the space group $Pnma$ with a Z value of four, and possesses an extended porous 3D framework in which the asymmetric unit contains one Sr atom, one ATA ligand, and one O^{2-} ion. The strontium(II) ion is eight-coordinated and binds six oxygen atoms from the carboxylate groups belonging to four ATA ligands (four chelating oxygen atoms O1, O1^{1#}, O2, and O2^{1#}; two *syn-syn* μ_2 -carboxylate oxygen atoms, O1^{2#} and O1^{3#}, in which 1# = $-\frac{1}{2} + x, y, \frac{1}{2} - z$; 2# = $-1 + x, y, z$; and 3# = $-1 + x, \frac{1}{2} - y, z$), and two μ_2 -O bridging oxide atoms (O8 and O8^{4#}, in which 4# = $-\frac{1}{2} + x, \frac{1}{2} - y, \frac{1}{2} - z$); the coordination environment is shown in Figure 1c). The position of the amino nitrogen atom in the benzene ring of ATA is disordered in two places with half occupancy. Each ATA anion bonds to four strontium(II) ions with the two carboxylate groups. Each carboxylate group chelates to one strontium atom through its oxygen atoms and one of the two oxygen atoms also bridges to another cation. SrO monocapped pentagonal bipyramids (Figure 1c) share edges to create an inorganic motif in the form of a zigzag 1D chain running along the a axis (Figure 1e). These 1D chains are connected by the μ links of the ATA ligands in two directions to generate the 3D framework (Figure 1d) with rhomboidal channels running along the a axis with a cross section of about $9 \text{ \AA} \times 18 \text{ \AA}$. The SAV value calculated by PLATON analysis was 412.7 \AA^3 , which was 29% of the unit cell volume. Therefore, channel blocking in Sr-MOF-1' probably results from DMF groups extending into the channels. Simplified topological analysis by TOPOS^[17] on compound Sr-MOF-1 revealed that this compound was a 2-

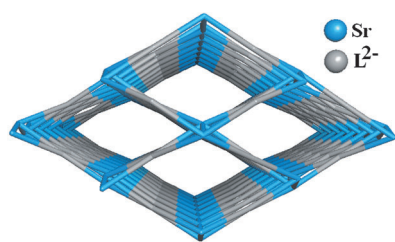


Figure 2. Simplified topological view of Sr-MOF-1, which shows a binodal 4,6-connected net topology.

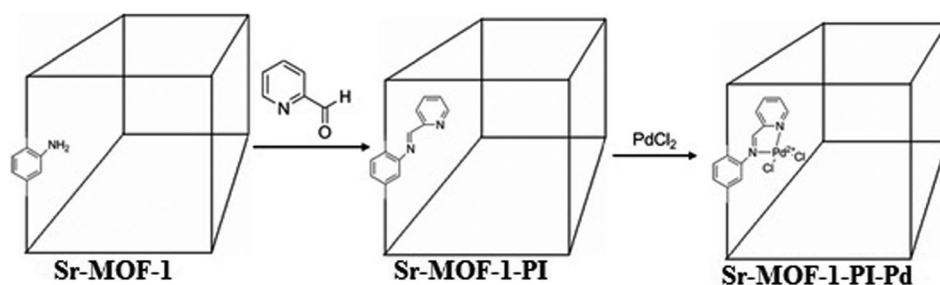
nodal 4, 6-c 3D net with the Schläfli symbol $\{3^2.6^2.7^2\}\{3^4.4^2.6^4.7^5\}$ (Figure 2, in which L^{2-} ligands act as a four-connected node and Sr(II) centers act as a six-connected node).

PSM of Sr-MOF-1

Sr-MOF-1 is a porous MOF decorated with pendant amine ($-NH_2$) groups on the walls of the pores. The amine moieties are not involved in the framework backbone, and therefore, are available to undergo chemical transformations. The free $-NH_2$ groups were thus covalently modified through a simple condensation reaction to produce a 2-pyridylimine ($R-N=C-C_5H_4N$) moiety, which was useful as a bidentate ligand. Pyridylimine formation activated the framework towards metal sequestering, as demonstrated by anchoring Pd^{II} to the wall of Sr-MOF-1. The preparative procedure is summarized in Scheme 1. To optimize the catalytic efficacy of Sr-MOF-1-PI-Pd, we controlled the functionalization by varying the amount of pyridine-2-aldehyde, and subsequently by varying the amount of palladium chloride in the Schiff base complex. Through this preparative method, a maximum functionalization of about 52% of the total $-NH_2$ groups was achieved without losing the framework integrity, whereas palladium complexation by the Schiff base complex was quantitative. The Schiff base complex features a square-planar geometry with a *cis* configuration, as described earlier.^[18] A similar type of ligand arrangement is expected in this case (Scheme 1).

Spectroscopic studies

The electronic spectrum of the catalyst Sr-MOF-1-PI-Pd was measured in the solid state (Figure S1 in the Supporting Infor-



Scheme 1. PSM procedure for obtaining MOFs containing a Pd^{II} Schiff base complex.

mation). The UV/Vis spectrum featured a strong band at $\lambda = 410$ nm that could be ascribed to the charge-transfer transition arising from π -electron interactions between the metal and ligand, which involves ligand to metal electron transfer that is typical for a Pd -Schiff base complex (Figure S1 in the Supporting Information).^[19] Other bands appearing in the region at $\lambda \approx 240$ and 300 nm can be attributed to intraligand transitions. The relatively weak band that appeared in the visible region for d-d transitions could not be resolved, owing to its very low extinction coefficient. The FTIR spectra of Sr-MOF-1, Sr-MOF-1-PI, and Sr-MOF-1-PI-Pd were measured as KBr pellets (Figure 3).

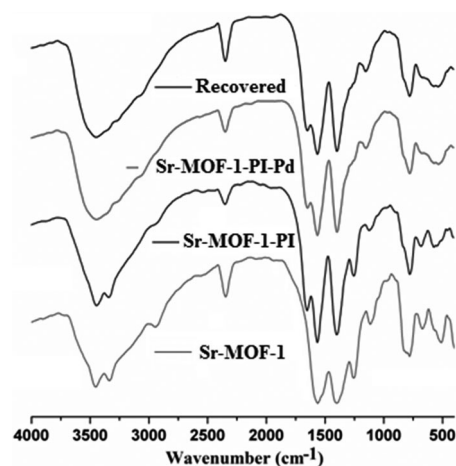


Figure 3. FTIR spectra of Sr-MOF-1, Sr-MOF-1-PI (after Schiff base formation), Sr-MOF-1-PI-Pd (after anchoring with Pd), and the recovered catalyst.

The characteristic IR vibration bands for free $-NH_2$ groups present in the framework of Sr-MOF-1 appeared in the range of $\tilde{\nu} = 3300$ – 3460 and 1500 – 1600 cm^{-1} . A moderately intense band for N–H stretching of Sr-MOF-1 appeared at $\tilde{\nu} \approx 3457$ cm^{-1} , whereas the relatively strong band that appeared at $\tilde{\nu} = 1555$ cm^{-1} could be ascribed to the bending vibration mode of the $-NH_2$ groups. The IR spectrum of Sr-MOF-1-PI shows a new band at $\tilde{\nu} = 1652$ cm^{-1} , in addition to the above-mentioned bands. This band can be ascribed to the vibration band for the azomethine group ($>C=N-$). The appearance of this new band in the IR spectrum of Sr-MOF-1-PI, which was absent in the case of Sr-MOF-1, clearly indicates that the Sr-MOF-1 framework has been organically modified, as shown in Scheme 1. It should be noted here that only 52% of $-NH_2$

groups undergo functionalization upon treatment with pyridine-2-aldehyde to form the Schiff base moiety in the framework (see above). In Sr-MOF-1-PI-Pd, the vibration bands for the azomethine group shift to a lower frequency range, which clearly indicates coordination of the azomethine nitrogen atom with palladium(II). Characteristic bands for the carboxylato vibra-

tion have appeared in the range $\tilde{\nu}=1250\text{--}1450\text{ cm}^{-1}$ in all samples.

Powder XRD studies

Powder XRD patterns of Sr-MOF-1', Sr-MOF-1, Sr-MOF-1-PI, and catalyst Sr-MOF-1-PI-Pd were studied (Figures S2 and S3 in the Supporting Information). A comparison of the powder XRD patterns of Sr-MOF-1, Sr-MOF-1-PI, and Sr-MOF-1-PI-Pd showed that the pattern of Sr-MOF-1 was not altered. This clearly shows that the framework structure of Sr-MOF-1 remained intact upon organic functionalization and metal complex formation. We also found that Sr-MOF-1 was stable in different solvents (Figure S4 in the Supporting Information).

Thermal measurements

Thermogravimetric (TG) analysis of Sr-MOF-1' and Sr-MOF-1 was performed by using a powdered sample under a nitrogen atmosphere in the temperature range from RT to 800 °C. The TG curve indicates that, upon heating, Sr-MOF-1' starts to lose coordinated DMF molecules at room temperature and this is complete at around 60 °C. The mass loss of 17% corroborates the theoretical value of 17%. Upon further heating, there was no mass change up to 330 °C, and thereafter, it rapidly started to lose mass in two continuous steps and was complete at around 500 °C. The mass loss seems to be due to continuous decomposition of the organic ligand present in the framework. For desolvated Sr-MOF-1, it does not show any mass loss between room temperature and 330 °C, then it also rapidly starts to lose mass, which is complete at around 686 °C, in two continuous steps and decomposes accordingly. Enhancement of the end point of decomposition may be due to greater stability of the desolvated framework (Figure S5 in the Supporting Information).

SEM and elemental mapping studies

SEM and X-ray elemental mapping were performed on samples Sr-MOF-1, Sr-MOF-1-PI, and Sr-MOF-1-PI-Pd (Figures S6 and S7 in the Supporting Information). Figure S6 in the Supporting Information displays the morphologies of all compounds. Figure S7 in the Supporting Information shows the presence of strontium in compound Sr-MOF-1 and, after it was postmodified by imine formation, the distribution of strontium ions within the material was similar. Figure S7c in the Supporting Information gives the distribution of palladium ions in the compound after palladium modification, and the distribution of palladium ions in the material was homogeneous. After the catalytic reaction, the strontium/palladium distribution in the compound is very similar to that of the parent material (Figure S7d in the Supporting Information). These results also suggest that palladium is not accumulated on the surface of the materials, but rather homogeneously dispersed.

Gas sorption studies

The nitrogen sorption isotherms of Sr-MOF-1, Sr-MOF-1-PI, catalyst Sr-MOF-1-PI-Pd, and the recovered catalyst are shown in Figure 4 and Figure S8 in the Supporting Information.

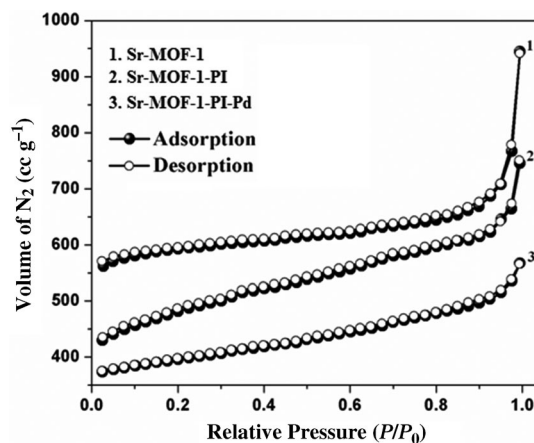


Figure 4. Nitrogen sorption isotherms of Sr-MOF-1; Sr-MOF-1-PI, and Sr-MOF-1-PI-Pd at 77 K.

All materials featured a type II isotherm (according to IUPAC nomenclature). The BET^[20] surface area of the materials was calculated from isotherms. The pore volume of the samples was calculated by using DFT methods. A gradual decrease in the BET surface area and pore volume was observed at each stage of modification. This is consistent with the fact that organic fragments or metal complexes occupy the pores upon modification of the MOF at different stages. Framework Sr-MOF-1 generates 3D rhombic channels with sizes of 9 Å × 18 Å, excluding van der Waals radii. The free void volume of Sr-MOF-1 is 29%, as estimated by PLATON.^[17] The nitrogen sorption study revealed that the BET surface area of Sr-MOF-1 was 2052 m²g⁻¹ (Langmuir surface area = 2859 m²g⁻¹; pore volume = 1.05 ccg⁻¹). Sr-MOF-1-PI showed a smaller N₂ uptake with a BET surface area of 1808 m²g⁻¹ (Langmuir surface area = 2578 m²g⁻¹; pore volume = 0.78 ccg⁻¹); this indicates that a Schiff base formed upon treatment with pyridine-2-aldehyde occupied space in the Sr-MOF-1 pores. Sr-MOF-1-PI-Pd showed the lowest N₂ uptake with a BET surface area of 1636 m²g⁻¹ (Langmuir surface area = 2397 m²g⁻¹) and pore volume of 0.69 ccg⁻¹; this demonstrates that the metal is anchored to the framework compound.

Recently, many modified MOFs have been developed for CO₂ adsorption based on our environmental concerns.^[21] To enhance adsorption, many techniques have been introduced to alter the MOF surface or metal nodes, such as introducing heteroatoms into the ligand systems, as well as anchoring an alkyl amine to the ligand arm or on the metal centers. Interactions between the lone pair of nitrogen and CO₂ have been very effective to enhance the gas adsorption ability. To date, three major classes of nitrogen-functionalized MOFs have been synthesized: N-heterocycle derivatives, aromatic amine

derivatives, and alkylamine-bearing frameworks.^[22] Among the established framework systems, aromatic amine containing linkers, and postmodified amino-functionalized MOFs are more efficient for their expected affinity of amino groups toward CO₂ and generated significant interest in aromatic amine functionalized frameworks.^[22–24] Amine functionalization enhanced the CO₂ capacity in a number of other MOFs, including Ni₂(NH₂-BDC)₂(DABCO) (BDC = 1,4-benzenedicarboxylate, DABCO = 1,4-diazabicyclo[2.2.2]octane), Al(OH)(NH₂-BDC), and In(OH)(NH₂-BDC), when comparing their low-pressure capacities with that of the parent material (Ni₂(BDC)₂(DABCO), Al(OH)(BDC), and In(OH)(BDC)).^[23e] At 298 K and 1 bar, Sr-MOF-1 adsorbs approximate 8.0 wt% CO₂ (Figure 5), which is signifi-

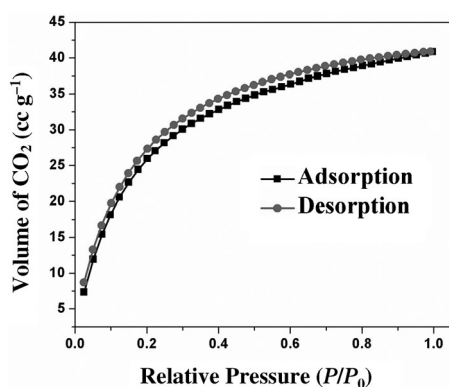


Figure 5. Carbon dioxide sorption isotherms of Sr-MOF-1 at 298 K and 1 bar.

cantly higher than that of its analogous zinc compound IRMOF-3 (CO₂ uptake is about 5.0 wt% at 298 K and 1.1 bar).^[23f]

On the other hand, it is noteworthy that Sr-MOF-1 shows a very good H₂ adsorption capability of 1.87 wt% at 77 K and 1 bar (Figure 6), which is significant and comparable to similar MOF families, for example, IRMOF-3 (the hydrogen uptake is about 1.42 wt% at 77 K and 1 bar).^[25] As a source of energy, hydrogen is a new hope for our modern civilization to replace depleted energy sources.^[26] The main goal is to develop an on-board H₂ storage system that fulfils successfully the daily need for fuel.^[27] As promising hydrogen storage materials, MOFs

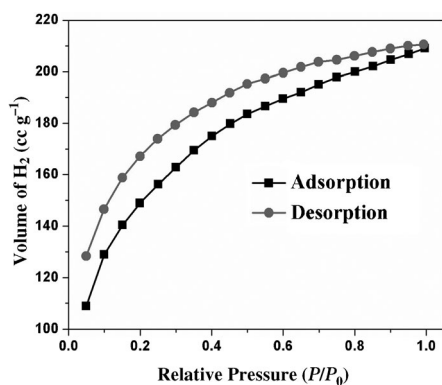


Figure 6. Hydrogen sorption isotherms of Sr-MOF-1 at 77 K and 1 bar.

have been extensively studied in the past decade. Several factors that influence the hydrogen uptake of porous MOFs, such as surface area, catenation, ligand functionalization, doping with alkali metals, and unsaturated metal centers, have been extensively studied.^[25] On the other hand, strontium(II) has a large coordination number, which varies from seven to ten. Therefore, it is very difficult to find a highly porous MOF containing strontium(II) in its metal site. Sr-MOF-1 is the first reported highly porous strontium(II) MOF, which exhibits the largest surface area with the highest low-pressure CO₂ and H₂ uptake among the strontium(II) MOF family.

Catalytic activity studies

Suzuki cross-coupling reaction

The catalytic activity of Sr-MOF-1-PI-Pd in the Suzuki cross-coupling reaction was first tested between bromobenzene and phenylboronic acid. Solvents and bases have remarkable influences on the reactivity of the catalyst in the Suzuki cross-coupling reaction; the results are summarized in Table 1 (more

Table 1. The effect of solvents and bases on Suzuki cross-coupling reactions.^[a,b]

Entry	Solvent (v/v)	Base	Time [min]	Yield ^[c] [wt%]
1	DMF	no base	90	28
2	DMF	K ₂ CO ₃	90	80
3	DMF/H ₂ O (4:1)	K ₂ CO ₃	10	100
4	DMF/H ₂ O (4:2)	K ₂ CO ₃	20	100
5	DMF/H ₂ O (4:3)	K ₂ CO ₃	40	100
6	H ₂ O	K ₂ CO ₃	90	36
7	MeOH	K ₂ CO ₃	90	52
8	EtOH	no base	90	18
9	EtOH	K ₂ CO ₃	90	68
10	EtOH/H ₂ O (4:1)	K ₂ CO ₃	90	100

[a] Reaction conditions: aryl halide (3 mmol), phenylboronic acid (3.3 mmol), base (3 mmol), Sr-MOF-1-PI-Pd catalyst (0.002 g; Pd content: 10.44×10^{-2} mol%, Pd/ArX molar ratio; 0.07:1) in solvent (5 mL) at 80 °C. [b] No homocoupled product was observed during the course of the reaction. [c] Yield determined by GC.

results are given in Table S1 in the Supporting Information).^[28] Preliminary screening of solvents revealed that the presence of DMF could efficiently catalyze the Suzuki cross-coupling reaction in water. Additionally, in DMF, the rate of reaction is very fast; however, palladium leaches from the solid catalyst, which is not desirable from environmental and economic points of view. Leaching of palladium was diminished with increasing H₂O/DMF ratio. It is well established that leaching of Pd often occurs in C–C coupling reactions if DMF is used as a solvent.^[29] Notably, for a desirable activity of catalyst Sr-MOF-1-PI-Pd can be achieved by using ethanol instead of DMF. The optimal conditions involved using K₂CO₃ as a base in 20% aqueous ethanol (Table 1, entry 10). Under the same conditions, NaHCO₃,

KHCO₃, NaOAc·3H₂O, KOAc, Na₃PO₄·12H₂O, and K₃PO₄·3H₃O gave moderate biphenyl yields (Table S1 in the Supporting Information, entries 1–9). Remarkably, when K₂CO₃ and Na₂CO₃ were used (Table 1, entry 10, and Table S1 in the Supporting Information, entry 3), good to excellent biphenyl yields were obtained, whereas K₂CO₃ in water gave only a 36% yield of biphenyl (Table 1, entry 6). The use of trialkylamine or lithium chloride as a base resulted in a low yield (Table S1 in the Supporting Information, entries 10 and 11). Indeed, K₂CO₃ in 20% aqueous ethanol was found to be the best choice, in view of an almost quantitative biphenyl yield obtained within a reasonably short reaction time (1.5 h; Table 1, entry 10).

In the Suzuki cross-coupling reaction, the catalytic activities of Sr-MOF-1-PI-Pd for various substrates were determined at 80 °C in air by using a suitable solvent (20% aqueous ethanol) and base (K₂CO₃). The results are summarized in Table 2.

Table 2. Suzuki cross-coupling reactions catalyzed by Sr-MOF-1-PI-Pd.^[a,b]

Entry	R ^[c]	X	Time [h]	Yield ^[d] [wt%]	TOF ^[e] [h ⁻¹]
1	H	I	2.0	100	719
2	H	Br	1.5	100	958
3	H	Cl	6	25	60
4	OH	Br	1.5	72	690
5	OMe	Br	1.5	78	747
6	NH ₂	Br	1.5	82	785
7	CHO	Br	1.5	96	919
8	COCH ₃	Br	1.5	100	958
9	NO ₂	Br	1	100	1437
10	CN	Br	1	94	1350
11	COOH	Br	3	74	354
12	Cl	Br	1.5	94	900
13	F	Br	1.5	100	958
14	NO ₂	Br	1.5	90	862

[a] Reaction conditions: aryl halide (3 mmol), phenylboronic acid (3.3 mmol), K₂CO₃ (3 mmol), Sr-MOF-1-PI-Pd catalyst (0.002 g; Pd content: 10.44 × 10⁻² mol%) in 20% H₂O/EtOH (5 mL) at 80 °C. [b] Homocoupled product was obtained only for Ar–Cl at a longer reaction time of 12 h. [c] All R groups are *para* substituted, except for entry 14 (R is *ortho* substituted). [d] Yield of product isolated/yield determined by GC. [e] TOF = turnover frequency in units of mol of biaryl per mol of Pd per h.

Among nonsubstituted aryl halides, iodo- and bromobenzene (Table 2, entries 1 and 2) showed comparable yields, which were higher than that of chlorobenzene. However, iodobenzene required a longer reaction time for 100% conversion (from GC analysis). Iodobenzene generally shows greater reactivity than bromobenzene in the cross-coupling reactions. Nevertheless, there were some exceptions in which reverse catalytic activity was observed in palladium-nanoparticle-based catalysts.^[30] In a recent study, it was proposed that I⁻ or

I₂ generated from iodobenzene could act as an inhibitor during the catalytic process.^[30b] The Sr-MOF-1-PI-Pd catalyst was capable of activating chlorobenzene (Table 2, entry 3), which normally remains unreactive in the C–C coupling reaction; however, the yield was much lower in comparison to some previous reports.^[31] Generally, it is difficult to activate C–Cl bonds because of their relative inertness.^[32] The *para*-substituted bromobenzene derivatives with –OH, –OCH₃, –NH₂, –CHO, –COCH₃, –NO₂, –COOH, –CN, –Cl, and –F groups generally show enhanced activity in Suzuki reactions. The reactivity of aryl bromides with electron-withdrawing substituents was higher than that of electron-donating substituents. It is worth noting that the turnover frequency (TOF) reached about 1437 h⁻¹ in the case of 4-nitrobromobenzene. However, aryl bromides containing the –COOH group required a longer reaction time for 100% conversion (from GC analysis) compared with other electron-withdrawing substituents. This may be due to a decrease in the basicity of the reaction medium. The chemoselectivity of the reaction was examined by using bromochlorobenzene (Table 2, entry 12). The sterically hindered *ortho*-substituted substrate *o*-nitrobromobenzene participated in the coupling reaction to give a good yield of product, 2-nitrobiphenyl (Table 2, entry 14). The kinetic profiles of the progress of catalytic reactions are shown in Figure 7. The rate of

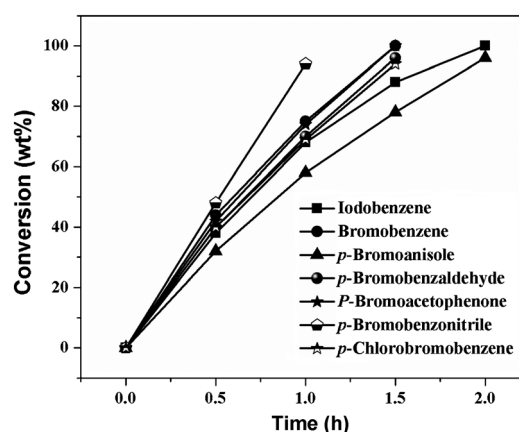
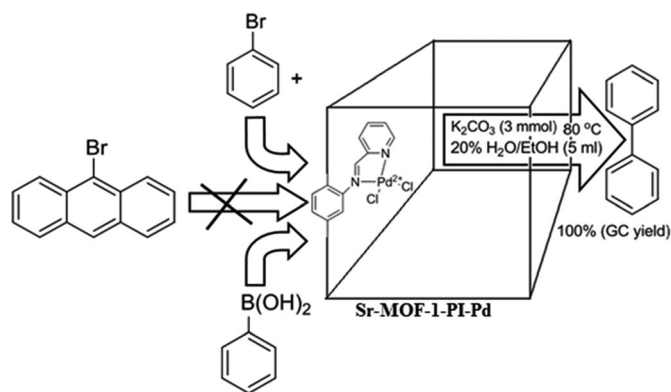


Figure 7. Kinetic plots for the Suzuki coupling reaction.

product formation increased steadily in the beginning of the reaction, giving no noticeable induction period. To ascertain if the coupling reaction was indeed occurring inside the pores of the catalyst Sr-MOF-1-PI-Pd, we performed a few control experiments with the bulkier substrate 9-bromoanthracene. The Suzuki reaction with 9-bromoanthracene yielded no coupling product and remained inactive (Scheme 2). This indicates that the functionalized pore windows of Sr-MOF-1-PI-Pd do not allow 9-bromoanthracene or its corresponding product to diffuse through the pores owing to their larger size.

Test for the homocoupling reaction

The homocoupling reaction sometimes features in the Suzuki reaction.^[33] Generally, the homocoupled product originates



Scheme 2. Test for shape selectivity with bromobenzene and 9-bromoanthracene. Reaction conditions: aryl halide (3 mmol), phenylboronic acid (3.3 mmol), base (3 mmol), Sr-MOF-1-PI-Pd catalyst (0.002 g) in 20% H₂O/EtOH (5 mL) at 80 °C.

from homocoupling among the boronic acid derivatives instead of coupling with the aryl halides. This phenomenon usually occurs due to the poor reactivity of the aryl halides and long reaction timescale. We examined this phenomenon by using Ph–Cl and Ph–Br with 4-methylphenylboronic acid, but we did not observe any 4,4'-dimethylbiphenyl when bromobenzene was used, and 4,4'-dimethylbiphenyl was obtained only in the case of chlorobenzene with longer reaction time (see the Supporting Information for product analysis). This result reveals typical behavior for less reactive Ph–Cl, which corroborates previous results^[34] and also supports the results obtained for cross-coupling reactions.

Separation and catalyst reuse

The catalyst Sr-MOF-1-PI-Pd is not thermal, air, or moisture sensitive and so there is no need to carry out the reaction under an inert atmosphere. The catalyst is easily recoverable by filtration and can be reused several times without any loss of catalytic activity. Because 2 mg of solid catalyst is not enough to recover, reuse, and finally characterize, the catalyst was collected from independent reactions of the same catalytic cycle and combined for the recycling study. The Suzuki coupling reaction was performed with bromobenzene under the same reaction conditions. After the first cycle of the reaction, the catalyst was recovered by centrifugation and then washed thoroughly with diethyl ether, followed by copious amounts of water to remove base present in the used catalyst, and finally with dichloromethane. The recovered catalyst was dried under vacuum at 100 °C overnight. Atomic absorption spectrometric analysis of the recovered catalysts confirmed that the palladium content of Sr-MOF-1-PI-Pd remained the same, even after its reuse. The performance of the recycled catalyst in the Suzuki coupling reaction in up to five successive runs is shown in Figure 8. The catalytic efficacy of the recovered catalyst remained almost the same in every run.

To check the stability of the catalyst, we characterized the recovered catalyst. After the catalytic reactions were over, solid catalyst was recovered by centrifugation and washed thor-

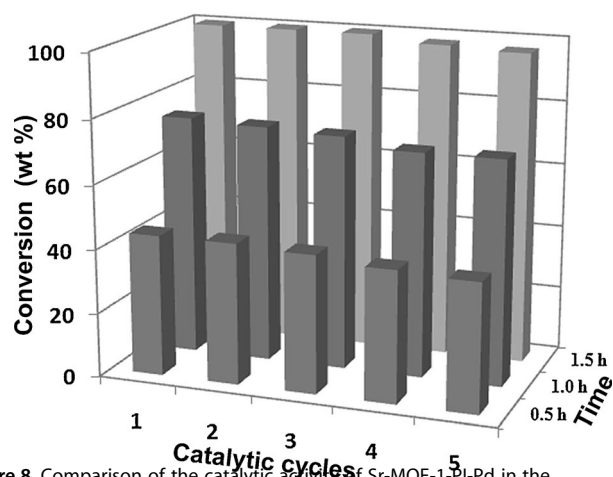


Figure 8. Comparison of the catalytic activity of Sr-MOF-1-PI-Pd in the Suzuki cross-coupling reaction between bromobenzene and phenylboronic acid in different catalytic cycles.

oughly as mentioned above and dried under vacuum at 100 °C overnight. The recovered catalyst was then subjected to powder XRD, IR spectral analysis, and gas adsorption studies. A comparison of the XRD patterns (Figure S3 in the Supporting Information), IR spectra (Figure 3), and results from gas adsorption studies (Figure S8 in the Supporting Information) of the pristine compound and recovered catalyst convincingly demonstrates that the structural integrity of the compound is retained after the reactions.

Heterogeneity test

To ascertain that the catalysis was indeed heterogeneous, we performed a series of tests, as described below.

Hot filtration test^[33]

To test whether metal was leaching from the solid catalyst during the reaction, the liquid phase of the reaction mixture was collected by filtration at the reaction temperature when the catalytic reaction (Suzuki) for bromobenzene was 30% complete and the residual activity of the supernatant solution was studied. After filtration of the Sr-MOF-1-PI-Pd catalyst from the batch reactor at the reaction temperature, coupling reactions do not proceed further. Atomic absorption spectrometric analysis (sensitivity up to 0.001 ppm) of the supernatant solution of the reaction mixture thus collected by filtration also confirmed the absence of palladium ions in the liquid phase. Thus, the results of the hot filtration test suggested that palladium was not being leached from the solid catalyst during cross-coupling reactions.

Solid-phase poisoning test

According to Richardson and Jones, the solid-phase poisoning test is one of the important tests to ascertain the true heterogeneity of the palladium-based catalyst in C–C coupling reactions.^[35] In this test, metal-free mercaptopropyl-functionalized

silica (in our case SH-SiO₂) was used as an effective palladium scavenger that selectively coordinated and deactivated leached palladium.^[35,36] Therefore, cessation of the reaction is expected if the coupling reaction is catalyzed by palladium species leached from the solid support. Richardson and Jones also observed that poisoning was effective when the S/Pd molar ratio was greater than 5.3:1. A comparison of the percentage conversion in C–C coupling reactions (Figure S9 in the Supporting Information) clearly indicates that the catalytic efficacy of Sr-MOF-1-PI-Pd was not affected when different amounts of SH-SiO₂ were added to the reaction mixture. In the coupling reaction, the catalyst remained active, even in the presence of a large excess of SH-SiO₂. Kinetic profiles of a typical Suzuki coupling reaction in the presence of the poisoning agent SH-

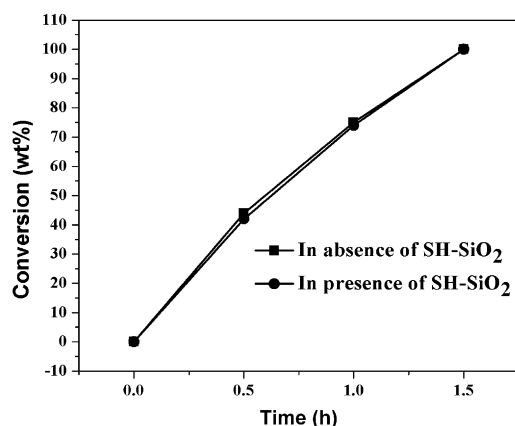


Figure 9. Kinetic profiles for the Suzuki coupling reaction of bromobenzene with or without SH-SiO₂ as the solid-phase poison (S/Pd ratio of 500:1).

SiO₂ (S/Pd ratio of 500:1) are shown in Figure 9. Notably, there was no induction period in these reactions with or without the poisoning agent.

Three-phase test^[33,34]

To ascertain whether the reactions were truly heterogeneous, we performed the three-phase test for the Suzuki reaction by using a designed aryl halide under standard conditions, as described in the Experimental Section (Scheme S1 in the Supporting Information). The compounds obtained through this process were *p*-phenylnitrobenzene and *p*-bromoacetophenone. The expected Suzuki product for *p*-bromoacetophenone, that is, *p*-phenylacetophenone was not detected. This clearly shows that *p*-bromoacetophenone has not participated in the coupling reaction while anchored on MCM-41. Should there be any leaching of palladium species from Sr-MOF-1-PI-Pd, anchored *p*-bromoacetophe-

none would have also participated in the above-described Suzuki reaction. However, this is not the case for the present catalyst. Therefore, all of these tests convincingly demonstrated that there was no leaching of Pd species during the Sr-MOF-1-PI-Pd-catalyzed C–C coupling reactions. A blank reaction was also performed, which showed that *p*-bromoacetophenone was also able to react with phenylboronic acid in the presence of *p*-nitrobromobenzene (Scheme S2 in the Supporting Information).

In search of MOF-based efficient heterogeneous catalysts for Suzuki reactions, several attempts have been made, of which a few deserve particular mention. Suzuki reactions catalyzed by various palladium-containing heterogeneous catalysts are given in Table 3. Different solid-supported palladium complexes were reported that catalyzed the Suzuki coupling reaction in environmental friendly water medium under truly heterogeneous conditions and catalysts were reused several times without any loss of activity.^[37] Corma et al. reported the Suzuki coupling of *p*-bromoanisole by a palladium-containing MOF in ethanol at 25 °C; this yielded *p*-methoxybiphenyl with high selectivity, but required a longer time (48 h) for a conversion of 87%.^[38] Štěpnička et al. studied the Suzuki coupling reaction of substituted bromobenzene with a reusable palladium catalyst prepared from mesoporous molecular sieves bearing nitrogen donor groups with different palladium loadings and, in some cases, a quantitative yield was obtained in anhydrous ethanol after 24 h of reaction.^[39] Palladium nanoparticles embedded in a porous sponge-like silica was used as a catalyst in the Suzuki coupling reaction of *p*-bromoanisole and phenylboronic acid, and up to 96% yield was obtained at a higher temperature (135 °C) in DMF. However, in this case, a gradual decrease in

Table 3. Suzuki reactions of aryl halides with phenylboronic acid catalyzed by different palladium catalysts.

Aryl halide	Catalyst	Yield [wt%]	Ref.
<i>p</i> -bromoacetophenone	oxime carbapalladacycle anchored to MCM-41	> 99 ^[a]	[34]
<i>p</i> -bromoacetophenone	oxime carbapalladacycle anchored to silica	> 99 ^[b]	[37]
<i>p</i> -bromoanisole	Pd-containing MOF	84 ^[c]	[38]
<i>p</i> -bromotoluene	Pd catalyst supported on mesoporous molecular sieves	quant. ^[d]	[39]
<i>p</i> -bromoanisole	Pd nanoparticles embedded in porous (4 nm) silica activated under H ₂	96 ^[e]	[40]
<i>p</i> -bromotoluene	phosphinoferrrocenyl carboxamides–Pd complex	100 ^[f]	[41]
bromobenzene	Pd-containing (0.1%–4.5%) basic zeolites	8–85 ^[g]	[42]
bromobenzene	Pd-containing (1%) basic zeolite	10 ^[h]	[42]
<i>p</i> -bromoacetophenone	Sr-MOF-1-PI-Pd	100 ^[i]	this study

[a] Water, 100 °C, <0.1 h. [b] Water, 100 °C, <0.1 h. [c] Ethanol, 25 °C, 48 h. [d] Ethanol, 75 °C, 24 h. [e] DMF, 135 °C, 24 h. [f] Ethanol–water, 80 °C, 16 h; [g] Ethanol/ethanol–water, 50 °C, 24 h. [h] Toluene, 50 °C, 24 h. [i] Ethanol–water, 80 °C, 1.5 h.

catalytic activity was observed in subsequent cycles.^[40] Štěpnička et al. also reported the Suzuki coupling of *p*-bromotoluene in ethanol/water catalyzed by a palladium complex of phosphinoferrrocenyl carboxamides bearing glycine pendant groups under homogeneous conditions with high yield and selectivity.^[41] Corma et al. observed palladium leaching in the Suzuki coupling reaction catalyzed by palladium-containing

basic zeolites in ethanol–water/ethanol medium and toluene was used as a solvent to avoid metal leaching.^[42] This is the major drawback of a heterogeneous catalytic system, in comparison to homogeneous counterparts. The present catalyst, Sr-MOF-1-PI-Pd, demonstrates a comparable efficiency in all of the reactions in terms of yield, cost, reaction time, selectivity, TOF, and reusability.

Conclusion

We succeeded in designing a novel amino-functionalized MOF based on strontium carboxylate. The compound underwent SC-to-SC transformation by desolvation to form a highly porous 3D MOF with pendant amines group for postfunctionalization. By postmodification, a new heterogeneous catalyst for carbon–carbon coupling reactions was developed by anchoring a Pd^{II} Schiff base moiety into the microporous Sr-MOF-1 catalyst. The catalyst showed a high activity towards the Suzuki cross-coupling reaction in environmentally friendly solvents (20% H₂O/EtOH and EtOH) under mild reaction conditions. The catalytic system tolerated a broad range of functional groups. The possibility of easy recycling of the catalyst and mild reaction conditions make the catalyst cheap and highly desirable to address environmental concerns. The gas adsorption capability also revealed promising results that could compete with well-established prototype MOFs; thus, Sr-MOF-1 is a novel addition to the MOF series based on alkaline-earth metals that can be postmodified and used as a heterogeneous catalyst.

Experimental Section

Synthesis of Sr-MOF-1'

Compound Sr-MOF-1' was prepared through the following procedure: Sr(NO₃)₂ (1.5 mmol, 316 mg) and 2-aminoterephthalic acid (1 mmol, 210 mg) was mixed in DMF (10 mL) and stirred for 1 h to form a light-yellow homogeneous solution, which was transferred into a 25 mL Teflon-lined autoclave and kept in a preheated oven at 160 °C for 3 days. After slow cooling to room temperature over a period of 6 h, block-shaped, light-yellow crystals were obtained (72% yield based on metal ion). The crystals were kept in the mother liquor. Elemental analysis calcd (%) for {Sr(ATA)(μ-DMF)}: C 38.85, H 3.52, N 4.11; found: C 39.14, H 3.89, N 4.82.

SC-to-SC transformation to prepare Sr-MOF-1

The crystals formed initially were removed from the mother liquor and washed with DMF and EtOH and dried under vacuum at 70 °C for 24 h. DMF molecules were removed during this period and the obtained desolvated crystals were kept for single-crystal X-ray analysis. Elemental analysis calcd (%) for {Sr₂(ATA)(μ-O)}: C 25.35, H 1.34, N 3.79; found: C 24.64, H 1.76, N 3.98.

Synthesis of Sr-MOF-PI [Sr₂(O)(ATA)_{1-x}(PITA)_x] (PITA = 2-pyridylimine terephthalate)

Pyridine-2-aldehyde (0.428 g, 4 mmol) was dissolved in dry CH₃CN (15 mL) before freshly prepared desolvated Sr-MOF-1 (1 g) was immersed, and the reaction mixture was allowed to stand for 15 days

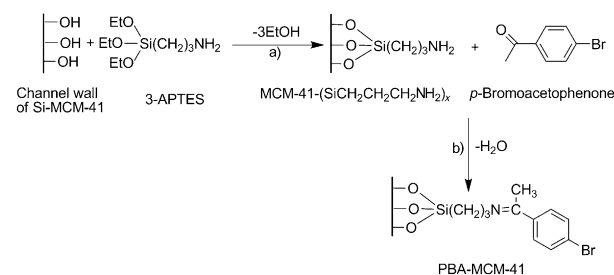
under an inert (nitrogen) atmosphere. After 15 days, the resulting pale-yellow solid was collected by centrifugation, washed with dry CH₃CN, and dried in vacuum at 120 °C. Elemental analysis was performed on samples outgassed under vacuum (120 °C, 12 h); elemental analysis calcd (%) for Sr₂(O)(ATA)_{0.48}(PITA)_{0.52} (corresponding to 52% amine functionalization): C 32.62, H 1.62, N 3.42; found: C 32.68, H 1.58, N 3.35.

Synthesis of Sr-MOF-PI-Pd [Sr₂(O)(ATA)_{1-x}(PITA-PdCl₂)_x]

Sr-MOF-PI-Pd was prepared by stirring desolvated Sr-MOF-1-PI (1 g) with (0.053 g, [PdCl₂] 0.3 mmol) in dry CH₃CN (15 mL) for 12 h under an inert (nitrogen) atmosphere. The brownish yellow solid thus formed was then filtered, dried in vacuum at 120 °C, and washed with CH₃CN by using Soxhlet extraction for 10 h to remove any unanchored palladium species and dried again in vacuum at 120 °C. Elemental analysis was performed on samples outgassed under vacuum (120 °C, 12 h); elemental analysis calcd (%) for Sr₂(O)ATA_{0.48}(PITA-PdCl₂)_{0.52} (corresponding to 52% amine functionalization and quantitative palladium uptake): C 26.63, H 1.32, N 2.79; found: C 26.67, H 1.28, N 2.73. The amount of Pd in the final solid was determined by atomic absorption spectrometry: calcd: Pd 11.03%; found: Pd 11.11% (10.44 × 10⁻² mol%).

Preparation of PBA-MCM-41

Anchoring of (3-aminopropyl)triethoxysilane (3-APTES) into MCM-41 was achieved by stirring MCM-41 (0.1 g) with 3-APTES (0.18 g, 0.81 mmol) in dry chloroform at RT for 12 h under a nitrogen atmosphere. The white solid MCM-41-(Si(CH₂CH₂CH₂NH₂)₂)_x thus produced was filtered and washed with chloroform and dichloromethane. This solid was then heated at reflux with *p*-bromoacetophenone (10 g, 50 mmol) in methanol (10 mL) for 3 h at 60 °C. The resulting yellowish solid PBA-MCM-41 was then collected by filtration and dried in a desiccator (Scheme 3).



Scheme 3. a) Organic modification of Si-MCM-41 with APTES/CHCl₃ and b) anchoring of *p*-bromoacetophenone onto MCM-41 (in ethanol).

CCDC 991451 and 991452 contain the supplementary crystallographic data for this paper. These data can be obtained free of charge from The Cambridge Crystallographic Data Centre via www.ccdc.cam.ac.uk/data_request/cif.

Acknowledgements

R.S. thanks the FCT for a post-doctoral grant (SFRH/BPD/71798/2010). The Portuguese group is financially supported by FEDER through the Programa Operacional Factores de Competitividade—COMPETE and national funds through the FCT—

Fundação para a Ciência e Tecnologia within CICECO project FCOMP-01-0124-FERDER-037271 (FCT Ref. Pest-C/CTM/LA0011/2013).

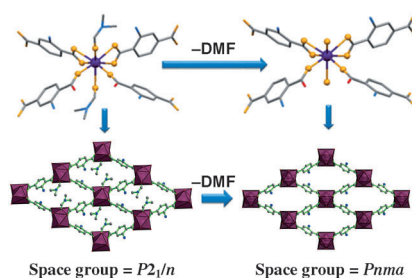
Keywords: cross-coupling · heterogeneous catalysis · metal-organic frameworks · strontium · structure elucidation

- [1] a) J.-R. Li, J. Sculley, H.-C. Zhou, *Chem. Rev.* **2012**, *112*, 869; b) S. Kitagawa, K. Uemura, *Chem. Soc. Rev.* **2005**, *34*, 109; c) H.-C. Zhou, J.-R. Li, O. M. Yaghi, *Chem. Rev.* **2012**, *112*, 673.
- [2] a) A. Corma, H. García, F. X. L. i Xamena, *Chem. Rev.* **2010**, *110*, 4606; b) J. Y. Lee, O. K. Farha, J. Roberts, K. A. Scheidt, S. B. T. Nguyen, J. T. Hupp, *Chem. Soc. Rev.* **2009**, *38*, 1450; c) M. A. Gotthardt, A. Beilmann, R. Schoch, J. Engelke, W. Kleist, *RSC Adv.* **2013**, *3*, 10676; d) M. A. Gotthardt, R. Schoch, T. S. Brunner, M. Bauer, W. Kleist, *ChemPlusChem* **2015**, *80*, 188–195.
- [3] a) M. Kurmoo, *Chem. Soc. Rev.* **2009**, *38*, 1353; b) Y.-F. Zeng, X. F.-C. Hu, X.-H. Bu, *Chem. Soc. Rev.* **2009**, *38*, 469; c) R. Liu, L. Li, X. Wang, P. Yang, C. Wang, D. Liao, J.-P. Sutter, *Chem. Commun.* **2010**, *46*, 2566; d) A. M. Ako, V. Mereacre, R. Clérac, W. Wernsdorfer, I. J. Hewitt, C. E. Anson, A. K. Powell, *Chem. Commun.* **2009**, 544; e) S. K. Langley, B. Moubaraki, K. S. Murray, *Dalton Trans.* **2010**, *39*, 5066; f) H. Miyasaka, M. Julve, M. Yamashita, R. Clérac, *Inorg. Chem.* **2009**, *48*, 3420.
- [4] a) W. Morris, B. Leung, H. Furukawa, O. K. Yaghi, N. He, H. Hayashi, Y. Houndonougbo, M. Asta, B. B. Laird, O. M. Yaghi, *J. Am. Chem. Soc.* **2010**, *132*, 11006; b) C. J. Doonan, W. Morris, H. Furukawa, O. M. Yaghi, *J. Am. Chem. Soc.* **2009**, *131*, 9492; c) H. Sato, R. Matsuda, K. Sugimoto, M. Takata, S. Kitagawa, *Nat. Mater.* **2010**, *9*, 661.
- [5] a) O. M. Yaghi, M. O’Keeffe, N. W. Ockwig, H. K. Chae, M. Eddaoudi, J. Kim, *Nature* **2003**, *423*, 705–714; b) H. Furukawa, K. E. Cordova, M. O’Keeffe, O. M. Yaghi, *Science* **2013**, *341*, 974 and references therein.
- [6] a) T. J. Colacot, *Platinum Met. Rev.* **2011**, *55*, 84–90 and references therein; b) L. Xue, Z. Lin, *Chem. Soc. Rev.* **2010**, *39*, 1692–1705; c) G. P. McGlacken, I. J. S. Fairiamb, *Eur. J. Org. Chem.* **2009**, 4011–4029; d) J. Muzart, *Tetrahedron* **2005**, *61*, 4179–4212.
- [7] a) N. Miyaoura, A. Suzuki, *Chem. Rev.* **1995**, *95*, 2457–2483; b) A. Suzuki, *J. Organomet. Chem.* **1999**, *576*, 147–168; c) J. K. Stille, *Angew. Chem. Int. Ed. Engl.* **1986**, *25*, 508–524; *Angew. Chem.* **1986**, *98*, 504–519.
- [8] B. M. Choudary, S. Madhi, N. S. Chowdari, M. L. Kantam, B. Sreedhar, *J. Am. Chem. Soc.* **2002**, *124*, 14127–14136.
- [9] a) D. Farrusseng, S. Aguado, C. Pinel, *Angew. Chem. Int. Ed.* **2009**, *48*, 7502–7513; *Angew. Chem.* **2009**, *121*, 7638–7649; b) C. Martínez, A. Corma, *Coord. Chem. Rev.* **2011**, *255*, 1558–1580; c) M. Ranocchiari, J. A. van Bokhoven, *Phys. Chem. Chem. Phys.* **2011**, *13*, 6388–6396; d) V. Calvino-Casilda, R. M. Martín-Aranda, *Recent Pat. Chem. Eng.* **2011**, *4*, 1–16.
- [10] a) W. Lu, Z. Wei, Z.-Y. Gu, T.-F. Liu, J. Park, J. Park, J. Tian, M. Zhang, Q. Zhang, T. Gentle, M. Bosch, H.-C. Zhou, *Chem. Soc. Rev.* **2014**, *43*, 5561–5593; b) W. Lu, D. Yuan, T. A. Makal, J.-R. Li, H.-C. Zhou, *Angew. Chem. Int. Ed.* **2012**, *51*, 1580–1584; *Angew. Chem.* **2012**, *124*, 1612–1616.
- [11] a) L. Yin, J. Liebscher, *Chem. Rev.* **2007**, *107*, 133–173; b) N. E. Leadbeater, M. Marco, *Chem. Rev.* **2002**, *102*, 3217–3274.
- [12] a) J. Juan-Alcañiz, J. Gascon, F. Kapteijn, *J. Mater. Chem.* **2012**, *22*, 10102–10118; b) J. S. Seo, D. Whang, H. Y. Lee, S. I. Jun, J. Oh, Y. J. Jeon, K. Kim, *Nature* **2000**, *404*, 982–986; c) Z. Wang, S. M. Cohen, *J. Am. Chem. Soc.* **2007**, *129*, 12368–12369.
- [13] A. Dhakshinamoorthy, H. García, *Chem. Soc. Rev.* **2012**, *41*, 5262–5284.
- [14] J. Huang, W. Wang, H. Li, *ACS Catal.* **2013**, *3*, 1526–1536 and references therein.
- [15] a) R. Sen, S. Bhunia, D. Mal, S. Koner, Y. Miyashita, K.-I. Okamoto, *Langmuir* **2009**, *25*, 13667–13672; b) R. Sen, R. Bera, A. Bhattacharjee, P. Gütllich, S. Ghosh, A. K. Mukherjee, S. Koner, *Langmuir* **2008**, *24*, 5970–5975; c) R. Sen, S. Koner, D. K. Hazra, M. Helliwell, M. Mukherjee, *Eur. J. Inorg. Chem.* **2011**, 241–248; d) R. Sen, D. K. Hazra, M. Mukherjee, S. Koner, *Eur. J. Inorg. Chem.* **2011**, 2826–2831.
- [16] a) R. Sen, D. Saha, S. Koner, *Chem. Eur. J.* **2012**, *18*, 5979–5986; b) D. Saha, R. Sen, T. Maity, S. Koner, *Dalton Trans.* **2012**, *41*, 7399–7408.
- [17] V. A. Blatov, A. P. Shevchenko, D. M. Proserpio, *Cryst. Growth Des.* **2014**, *14*, 3576–3586.
- [18] P. Pelagattia, M. Carcellia, M. Costab, S. Ianellia, C. Pelizzia, D. Rogolinoa, *J. Mol. Catal. A* **2005**, *226*, 107–110.
- [19] Y. Fan, W. You, W. Huang, J.-L. Liu, Y.-N. Wang, *Polyhedron* **2010**, *29*, 1149–1155.
- [20] S. Brunauer, P. H. Emmett, E. Teller, *J. Am. Chem. Soc.* **1938**, *60*, 309.
- [21] a) D.-X. Xue, A. J. Cairns, Y. Belmabkhout, L. Wojtas, Y. Liu, M. H. Alkordi, M. Eddaoudi, *J. Am. Chem. Soc.* **2013**, *135*, 7660–7667; b) K. Sumida, M. D. Rogow, J. A. Mason, T. M. McDonald, E. D. Bloch, Z. R. Herm, T.-H. Bae, J. R. Long, *Chem. Rev.* **2012**, *112*, 724–781.
- [22] a) N. Planas, A. L. Dzubak, R. Poloni, L.-C. Lin, A. McManus, T. M. McDonald, J. B. Neaton, J. R. Long, B. Smit, L. Gagliardi, *J. Am. Chem. Soc.* **2013**, *135*, 7402–7405; b) T. M. McDonald, W. R. Lee, J. A. Mason, B. M. Wiers, C. S. Hong, J. R. Long, *J. Am. Chem. Soc.* **2012**, *134*, 7056–7065.
- [23] a) J. An, S. J. Geib, N. L. Rosi, *J. Am. Chem. Soc.* **2010**, *132*, 38–39; b) R. Vaidhyanathan, J. Liang, S. S. Iremonger, G. K. H. Shimizu, *Supramol. Chem.* **2011**, *23*, 278–282; c) Y. E. Cheon, J. Park, M. P. Suh, *Chem. Commun.* **2009**, 5436–5438; d) R. Vaidhyanathan, S. S. Iremonger, K. W. Dawson, G. K. H. Shimizu, *Chem. Commun.* **2009**, 5230–5232; e) B. Arstad, H. Fjellvåg, K. O. Kongshaug, O. Swang, R. Blom, *Adsorption* **2008**, *14*, 755–762; f) A. R. Millward, O. M. Yaghi, *J. Am. Chem. Soc.* **2005**, *127*, 17998.
- [24] W. Lu, J. Sculley, D.-Q. Yuan, R. Krishna, H.-C. Zhou, *J. Phys. Chem. C* **2013**, *117*, 4057–4061.
- [25] J. L. C. Rowsell, O. M. Yaghi, *J. Am. Chem. Soc.* **2006**, *128*, 1304–1315.
- [26] M. P. Suh, H. J. Park, T. K. Prasad, D.-W. Lim, *Chem. Rev.* **2012**, *112*, 782–835.
- [27] L. Schlapbach, A. Züttel, *Nature* **2001**, *414*, 353–358.
- [28] a) S. Y. Gao, Z. L. Zheng, J. Lü, R. Cao, *Chem. Commun.* **2010**, 46, 7584–7586; b) M. Trilla, R. Pleixats, M. W. C. Man, C. Bied, J. J. E. Moreau, *Adv. Synth. Catal.* **2008**, *350*, 577–590; c) M. Lombardo, M. Chiarucci, C. Trombini, *Green Chem.* **2009**, *11*, 574–579; d) H. Hagiwara, K. H. Ko, T. Hoshi, T. Suzuki, *Chem. Commun.* **2007**, 2838–2840; e) Z. Guan, J. Hu, Y. Gu, H. Zhang, G. Lia, T. Li, *Green Chem.* **2012**, *14*, 1964–1970; f) J. Z. Zhang, W. Q. Zhang, Y. Wang, M. C. Zhang, *Adv. Synth. Catal.* **2008**, *350*, 2065–2076.
- [29] D. Astruc, *Inorg. Chem.* **2007**, *46*, 1884–1894.
- [30] a) K. Shimizu, T. Kan-no, T. Kodama, H. Hagiwara, Y. Kitayama, *Tetrahedron Lett.* **2002**, *43*, 5653–5655; b) A. Primo, M. Liebel, F. Quignard, *Chem. Mater.* **2009**, *21*, 621–627.
- [31] a) V. Calò, A. Nacci, A. Monopoli, F. Montingelli, *J. Org. Chem.* **2005**, *70*, 6040–6044; b) S. Bhunia, R. Sen, S. Koner, *Inorg. Chim. Acta* **2010**, *363*, 3993–3999.
- [32] a) J. Zhou, X. Guo, C. Tu, X. Li, H. Sun, *J. Organomet. Chem.* **2009**, *694*, 697–702; b) M. Nonnenmacher, D. Kunz, F. Rominger, T. Oeser, *J. Organomet. Chem.* **2007**, *692*, 2554–2563; c) H. Yang, X. Han, Z. Ma, R. Wang, J. Liu, X. Ji, *Green Chem.* **2010**, *12*, 441–451.
- [33] A. Corma, D. Das, H. García, A. Leyva, *J. Catal.* **2005**, *229*, 322–331.
- [34] C. Baleizão, A. Corma, H. García, A. Leyva, *J. Org. Chem.* **2004**, *69*, 439–446.
- [35] J. M. Richardson, C. W. Jones, *J. Catal.* **2007**, *251*, 80–93.
- [36] J. D. Webb, S. MacQuarrie, K. McEleney, C. M. Crudden, *J. Catal.* **2007**, *252*, 97–109.
- [37] C. Baleizão, A. Corma, H. García, A. Leyva, *Chem. Commun.* **2003**, 606–607.
- [38] F. X. Llabrés i Xamena, A. Abad, A. Corma, H. García, *J. Catal.* **2007**, *250*, 294–298.
- [39] J. Demel, M. Lamač, J. Čejka, P. Štěpnička, *ChemSusChem* **2009**, *2*, 442–451.
- [40] G. Budroni, A. Corma, H. García, A. Primo, *J. Catal.* **2007**, *251*, 345–353.
- [41] J. Tauchman, I. Cisařová, P. Štěpnička, *Organometallics* **2009**, *28*, 3288–3320.
- [42] A. Corma, H. García, A. Leyva, *Appl. Catal. A* **2002**, *236*, 179–185.

Received: October 16, 2014
Published online on ■■■■■, 0000

FULL PAPER

Expanding on the bare essentials: A novel amino-functionalized strontium metal-organic framework (Sr-MOF) has been synthesized that undergoes single-crystal to single-crystal transformation to become a microporous MOF (see figure). Palladium(II) has been anchored onto the arm of the framework and the obtained compound has been used in the Suzuki cross-coupling reaction. The high efficiency of the catalyst remains unaltered after five successive cycles.

**Heterogeneous Catalysis**

R. Sen,* D. Saha, S. Koner, P. Brandão,
Z. Lin*



Single Crystal to Single Crystal (SC-to-SC) Transformation from a Nonporous to Porous Metal–Organic Framework and Its Application Potential in Gas Adsorption and Suzuki Coupling Reaction through Postmodification

